Bispectrum of Stator Phase Current for Fault Detection of Induction Motor

Juggrapong Treetrong, Jyoti K. Sinha*

School of Mechanical, Aerospace and Civil Engineering,
The University of Manchester, Seckville Street, P.O Box 88, M60 1QD, UK

Fengshou Gu, Andrew Ball
School of Computing and Engineering
The University of Huddersfield, Queensgate, Huddersfield HD1 3DH, UK

Abstract

The number of research studies have shown that the fault in the stator or rotor generally show sideband frequencies around the mains frequency (50Hz) and it higher harmonics in the spectrum of the Motor Current Signature Analysis (MCSA). However in the present experimental studies such observations have not been identified, but any fault either in the stator or the rotor may distort the sinusoidal response of the motor speed and the main frequency so the MCSA response may contain number of harmonics of the motor speed and the mains frequency. Hence the use of the higher order spectrum (HOS), namely the bisepctrum of the MCSA has been proposed here because it relates both amplitude and phase of number of harmonics in a signal. It has been observed that it not only detects the early fault but also indicate the severity of the fault to some extent.

*Corresponding author

Email: Jyoti.Sinha@manchester.ac.uk

1.0. Introduction

Induction motors are the most widely used motors among different electric motors because of their high level of reliability, efficiency and safety. However, these motors are often exposed to hostile environments during operation which leads to early deterioration leading to the motor failure. It has also been observed that 30-40% of all recorded faults are generally related to the stator or armature faults caused due to the shorting of stator phase winding and 5-10% fault related to the rotor (broken bar and/or end ring fault) [1]. Hence the condition monitoring technique has generally been used to detect the fault at the early stage so that the remedial action can be done in much planned way to reduce the machine downtime and to maintain the overall plant safety.

Motor Current Signature Analysis (MCSA) is one of the most spread procedures for health monitoring of the motor since decades. One of the main reasons for using this method is that the other methods require invasive access to the motor and they also need extra equipment/sensors for measuring the required signals. The research has been progressed in mainly two directions using the stator phase current and voltage signals – the detection of faults [1-12] and the quantification of the faults by the motor parameters estimation [13-18]. First one is important for the quick health assessment on routine basis, however the later one useful to know the extent of the faults so that remedial action can be done quickly. There are number of the research studies that have used the spectrum of the stator phase current signal for stator fault [8-12] and the rotor fault [2-7], often based on the presence of the side band frequency (related to the slip frequency) and its harmonics around the power supply frequency or/and its harmonics. However in the present experiments, the side bands were not clearly seen for both rotor and stator faults in their spectra with frequency resolution of 1.25Hz when using the motor stator phase current signals, hence the use of the Higher Order Spectrum (HOS) [19-20] has been applied on the stator phase current signal instead of the spectrum. It is because the any fault in the motor expected to generate harmonic components of the motor RPM and the mains frequency in the motor current signal so the relation between different harmonic components in the signal has been exploited using the HOS, namely the bispectrum, which has been observed to be useful in detection and identification of the rotor and stator faults. The paper discusses the concept of the bispectrum and the presents the bispectrum results of the experimental cases of the induction motor with the healthy, stator winding short-circuits (stator fault) and broken rotor bars (rotor fault) conditions.

2.0. Higher Order Spectra (HOS)

The n^{rd} order moment function of a signal, $x(t)$ is defined as,

$$\mathbf{R}_{xxxx.....x}(\tau_1,\tau_2,\tau_3,.....,\tau_n) = E[x(t)x(t-\tau_1)x(t-\tau_2)x(t-\tau_3)......x(t-\tau_n)], \quad (1)$$

where $E[.]$ denotes the expectation operator, and τ as delay. The Power Spectral Density (PSD) is defined as the Fourier Transformation (FT) of a 2^{nd} order moment function of Equation (1), and is computed as

$$\text{PSD, } \mathbf{S}_{xx}(f_k) = E[\mathbf{X}(f_k)\mathbf{X}^*(f_k)],\ k = 1, 2, 3, \ldots, N \quad (2)$$

where $\mathbf{S}_{xx}(f_k)$ is the PSD, $\mathbf{X}(f_k)$ and $\mathbf{X}^*(f_k)$ are the DFT and its complex conjugate at frequency f_k for the time series $x(t)$. N is the number of the frequency points. E[.] denotes the mean operator here. Let us assume that the time domain signal, $x(t)$, of the time length equals to t. This time signal has been divided into n number of segments with some overlap and each segment contains 2N number of data points with sampling frequency, f_s Hz. If $X_r(f_k)$ is the FT of the rth segment, $x_r(t)$, at the frequency, f_k, then the averaged or mean PSD can be computed as

$$\mathbf{S}_{xx}(f_x) = \frac{\sum_{r=1}^{n} X_r(f_k)X_r^*(f_k)}{n}, \quad (3)$$

where $f_k = (k-1)df$, $df = \dfrac{f_s}{2N}$

The PSD gives only the content of different frequencies and their amplitudes in a signal. However, the HOS – Bispectrum and Trispectrum provide insights into non-linear coupling between frequencies (as it involves both amplitudes and phases) of a signal compared to the traditional PSD. For example, the Bispectrum is the double FT of a 3^{rd} order moment of a time signal [19-20] that involves two frequencies components (both amplitudes and phases) of the signal together with a frequency component summation of first two frequencies, and is mathematically expressed as

$$\mathbf{B}_{xxx} = \int_{-\infty}^{+\infty}\int_{-\infty}^{+\infty} \mathbf{R}_{xxx}(\tau_1, \tau_2) e^{-j2\pi(f_1\tau_1 + f_2\tau_2)} d\tau_1 d\tau_2, \tag{4}$$

where $\mathbf{R}_{xxx}(\tau_1, \tau_2) = E[x(t)x(t-\tau_1)x(t-\tau_2)]$ is the 3^{rd} order moment, and the Bispectrum is computed by the signal DFT as

$$\text{Bispectrum, } \mathbf{B}(f_l, f_m) = E[\mathbf{X}(f_l)\mathbf{X}(f_m)\mathbf{X}^*(f_l + f_m)], \quad f_l + f_m \le f_N \tag{5}$$

$$\mathbf{B}(f_l, f_m) = \frac{\sum_{r=1}^{n} \mathbf{X}_r(f_l)\mathbf{X}_r(f_m)\mathbf{X}_r^*(f_l + f_m)}{n} \tag{6}$$

The Bispectrum is complex and interpreted as measuring the amount of coupling between the frequencies at f_l, f_m, and $f_l + f_m$, and is described by ‘quadratic phase coupling’. It has been assumed that if the frequencies, f_l and f_m are the p th and q th harmonics of the motor RPM then the component of the bispectrum, $B(f_l, f_m)$ has been represented as B_{pq} for better understanding.

3.0. Experiment Study

The schematic of the test rig is shown Figure 1. The test rig consists of an induction motor (4kW, 1400RPM) with load cell with a facility to collect the 3-phase current data directly to the PC at the user define sampling frequency. The experiments were conducted for these 3 different conditions – Healthy, Stator Fault and Rotor Faults at different load conditions. The data were collected at the sampling frequency of 1280 samples/s. The stator fault was simulated by the short circuits - 5 turn shot circuit, 10 turn short circuit and 15 turn short circuit whereas the rotor fault by the broken rotor bars. Table 1 gives the level of faults in the stator and the rotor [18].

Table 1 The level of faults in the stator and the rotor

100% Load	R_s	x_{ls}	R_r	x_{lr}	x_m
Healthy	1.5766	0.9170	0.9577	0.8795	40.0879
5 Turn Short	0.9104	0.6554	0.9934	0.8370	40.2341
10 Turn Short	0.5640	0.4944	0.9671	0.8297	40.1754
15 Turn Short	0.3046	0.2896	0.9473	0.8534	40.0233
Broken Bars	1.5500	0.9257	1.3730	1.2678	40.0223

Unit: Ohm (Ω)

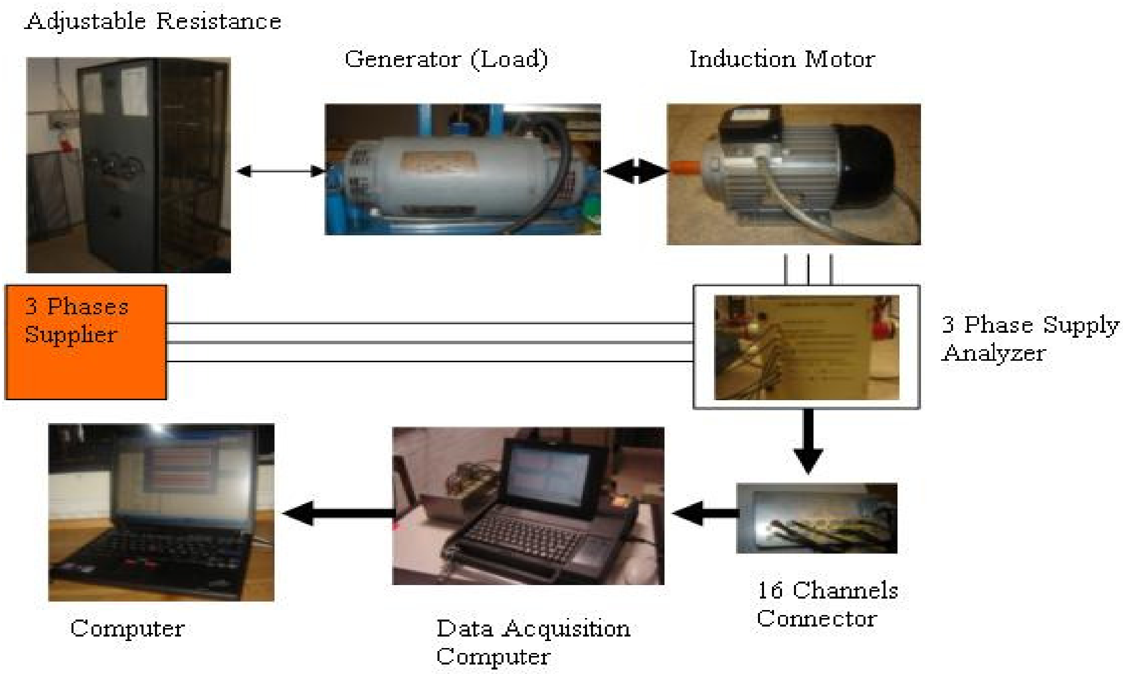

Figure 1 Schematic of the test rig

4.0. Data Analysis

A typical current plot for the healthy motor operating at 100% load is shown in Figure 2. The rated current for the motor is close to 10 Ampere. The amplitude spectra and the bispectra have also been estimated for all the experimental data. The frequency resolution was kept 1.25Hz with 90% overlap and number of average 82 for all the signal processing. The computation time using the Pentium-IV PC for both the spectrum and bispectrum was less than 30s which is definitely quick process for the health monitoring purpose. Few typical plots for the amplitude spectra and the bispectra at full load condition are shown in Figures 3-8.

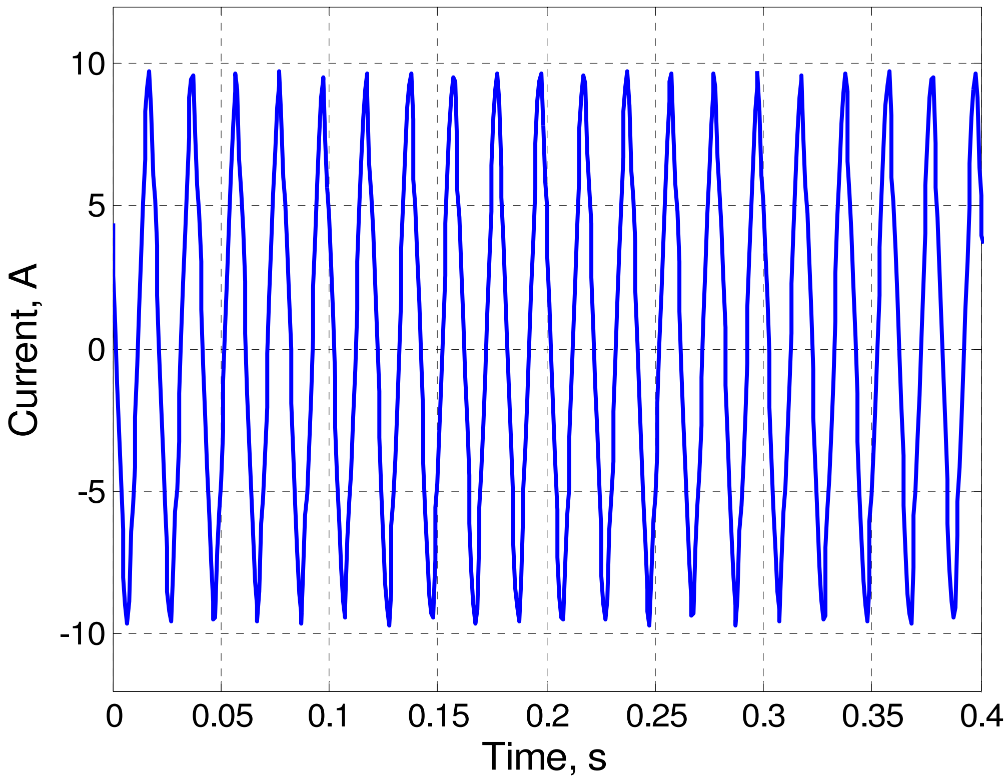

Figure 2 A typical current signal

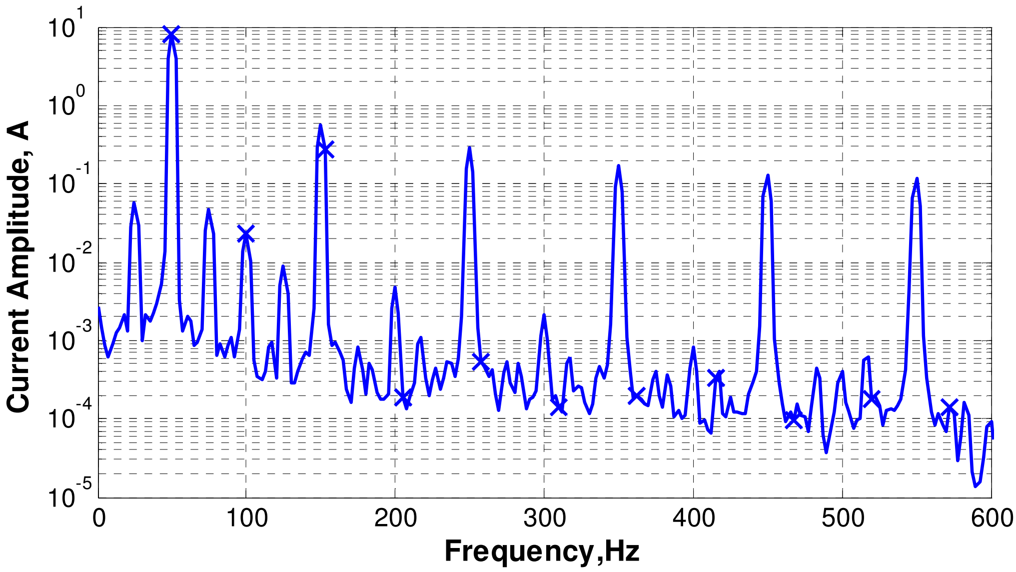

Figure 3 The spectrum of the stator phase current for the healthy motor

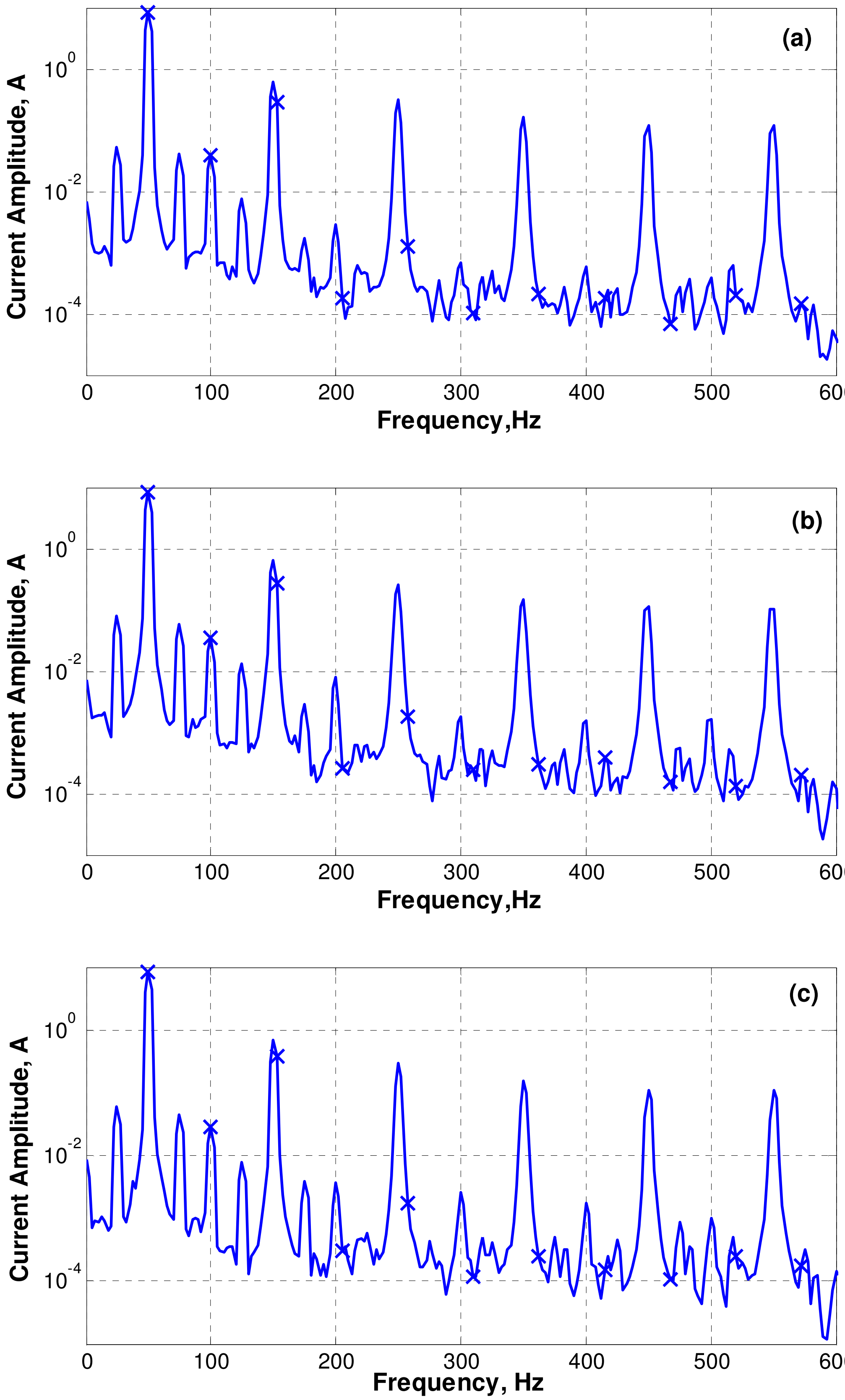

Figure 4 The spectra of stator phase current: (a) 5 turns short circuit, (b) 10 turns short circuit, and (c) 15 turns short circuit

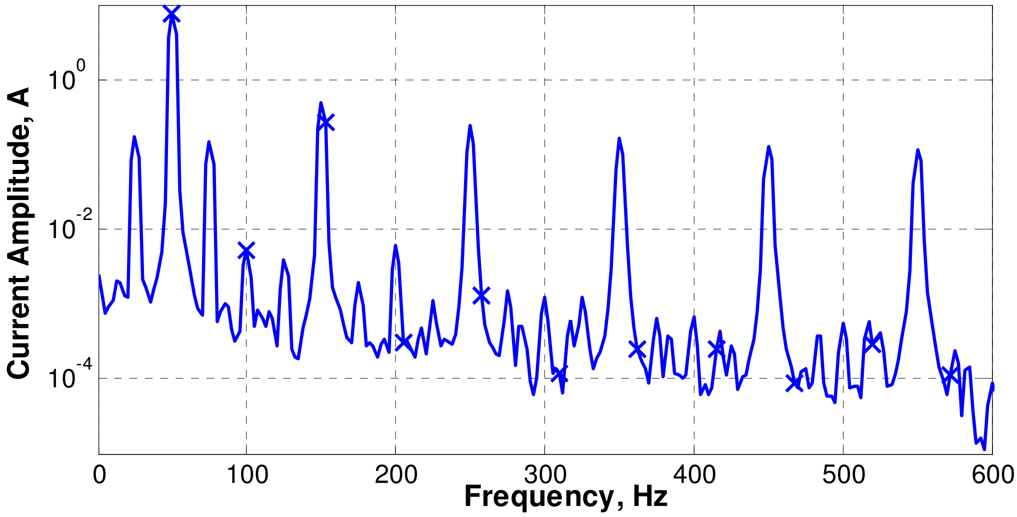

Figure 5 The spectrum of the stator phase current for the broken rotor bars motor

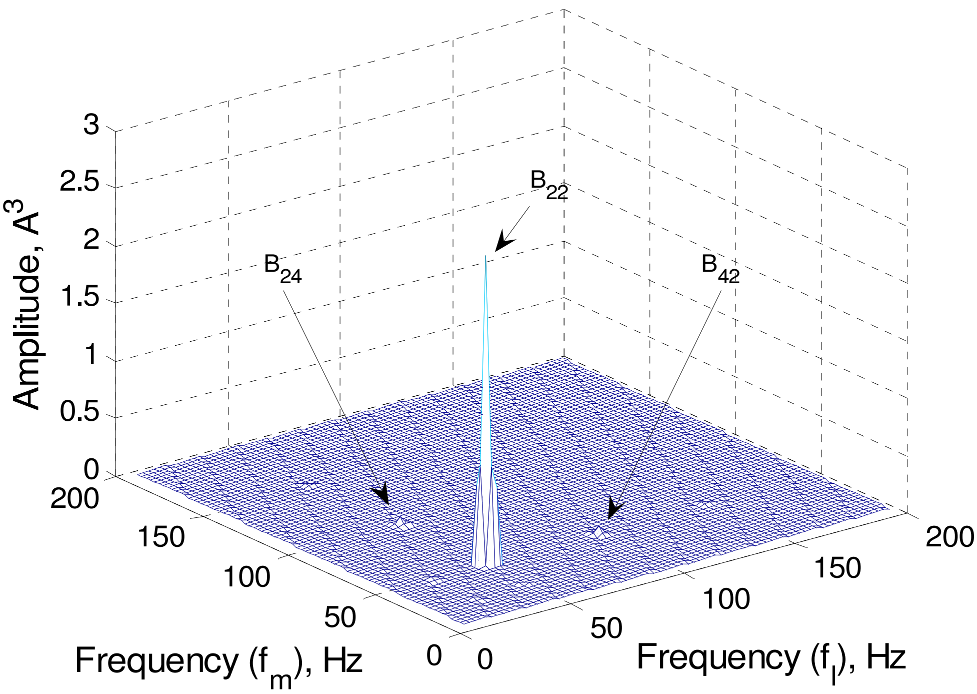

Figure 6 The bispectrum of the stator phase current for the healthy motor

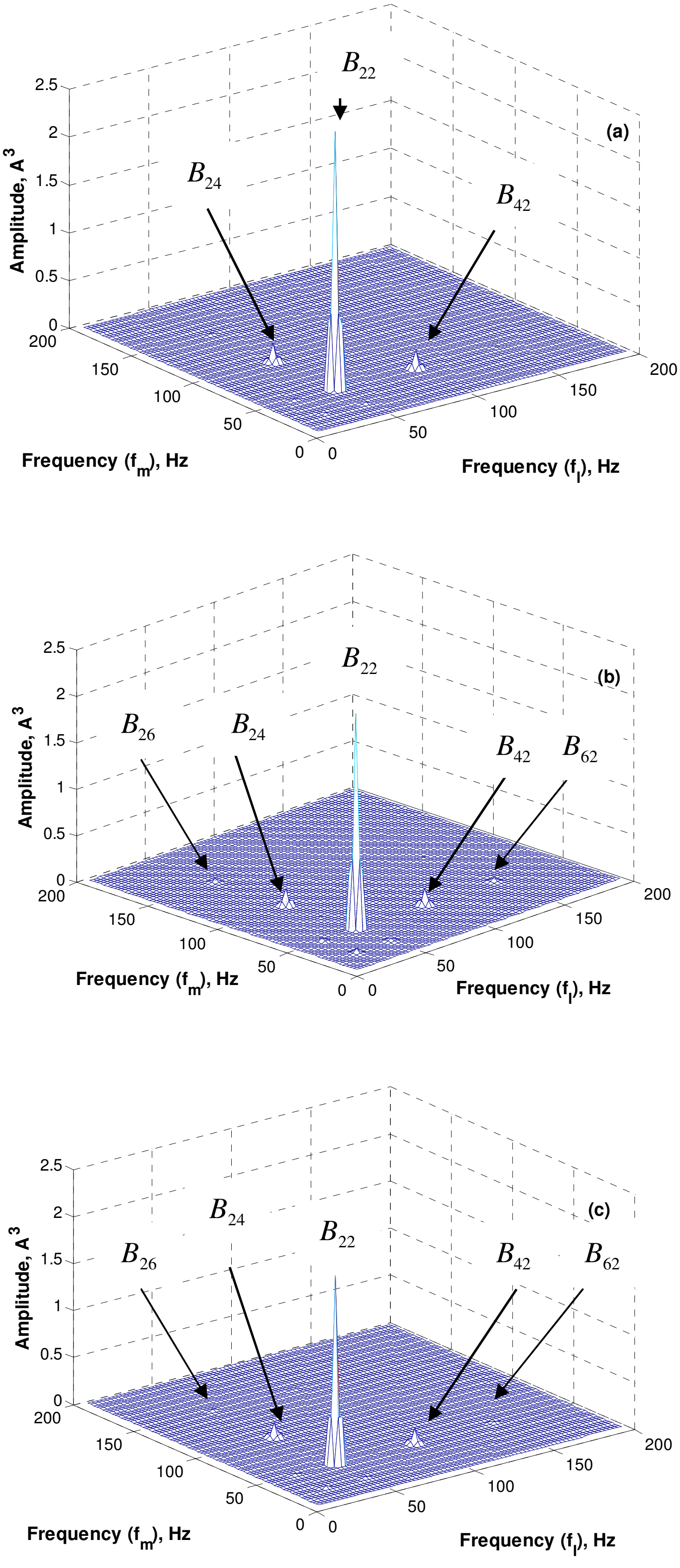

Figure 7 The bispectra of the stator phase current: (a) 5 Turns Short Circuit, (b) 10 Turns Short Circuit, and (c) 15 Turns Short Circuit

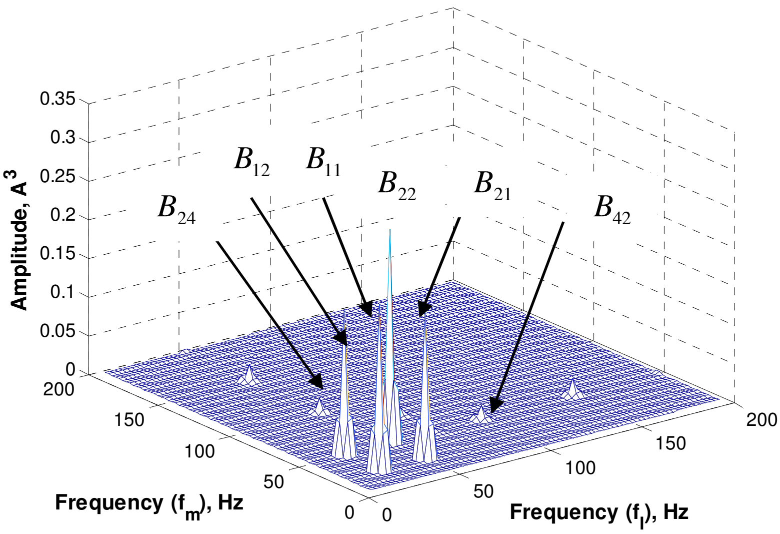

Figure 8 The bispectrum of the stator phase current for the broken rotor bars motor

4.1. Discussion

As can be seen from Figures 3-5, it is difficult to identify the faults based on the spectra with the frequency resolution of 1.25Hz of the current signals. All spectra almost look identical. In all cases, machine RPM (1x component) and its higher harmonics (2x, 3x,…) are present and no side band frequency at the main frequency related to the slip frequency has been seen to identify the fault as suggested in the earlier studies. The amplitude demodulation at a frequency for any signal removes that frequency, but modulated frequencies can be clearly identified from the demodulated signal. Hence here also, the amplitude demodulation at the mains frequency, 50Hz has been carried out for the phase current signals for the faulty rotor and stator conditions. The amplitude spectra of all the demodulated signals have shown only a single peak at the RPM of the motor. A typical such spectrum is shown in Figure 9 for the faulty rotor condition. Here again, the spectrum is not showing any peaks other than machine RPM which indicates that the frequency related to the slip frequency due to fault was not present in the current signal and so the identification just based on side-band was not possible for the present experimental cases.

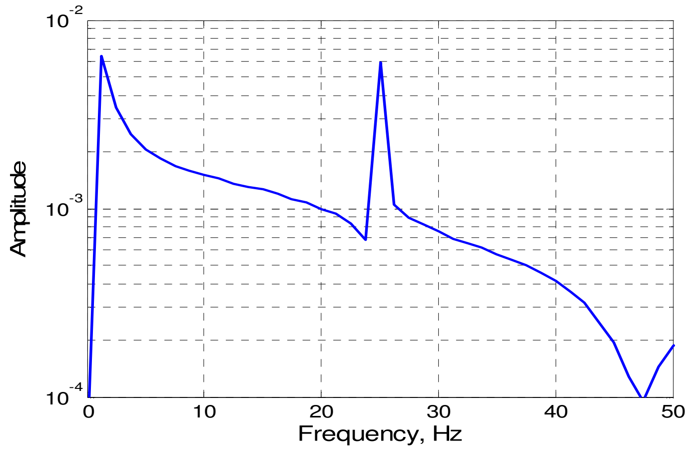

Figure 9 The spectrum of the amplitude demodulated stator phase current at mains frequency for the broken rotor bars motor

However, the bispectra of stator phase currents from the 3 different motor conditions seem to identify the faults as can be seen in Figures 6-8. The peaks in the bispectra plots are indicated by B_{11}, B_{12}, B_{21} and so on. Here B_{11} means the relation of 1x, 1x and 2x components, $B_{12}(=B_{21})$ the relation of 1x, 2x and 3x (1x+2x) components in a signal.

In the bispectrum, the only significant peak B_{22} has been seen for the healthy motor condition. However, the for the faulty stator cases the amplitude of the bisepctrum component, B_{22}, decreases as the level of the stator fault increases and the significant increase in the amplitude of the bispectrum component, B_{24} $(=B_{42})$ compared to the healthy condition, nearly 2.4 times. Other peaks, B_{11}, B_{12} $(=B_{21})$ and B_{26} $(=B_{62})$ observed to remain comparable with the amplitudes for the healthy condition (Figures 6-7). However, in case of the faulty rotor case the peak, B_{22}, reduced significantly from the healthy condition (nearly 0.10 times) and the faulty stator cases, but other peaks, B_{11}, B_{12} $(=B_{21})$ increased significantly (nearly 8-10 times) compared to the healthy and the stator fault cases. These observations are also summarized in Table 2. Hence the based on the observation, it can be concluded that the bispectrum of the phase current signal can identify and distinguish the rotor fault and stator fault of the electric motor. It has also been observed that the amplitude of the peaks can show the severity of the stator and the rotor faults.

To confirm the robustness of the proposed study, the tests were conducted for different load levels of the motor. The observation made in the bispectrum at 100% motor load for the healthy, the stator fault and the rotor fault cases was consistent with the different load conditions. Figure 10 shows the typical cases for the rotor fault at no load, 25% load, 50% load and 75% load where it can be seen that the appearance of peaks in the bisepctra at different loads is consistent with the bispectrum shown in Figure 8, hence method seems to be robust for the fault detection in the motor.

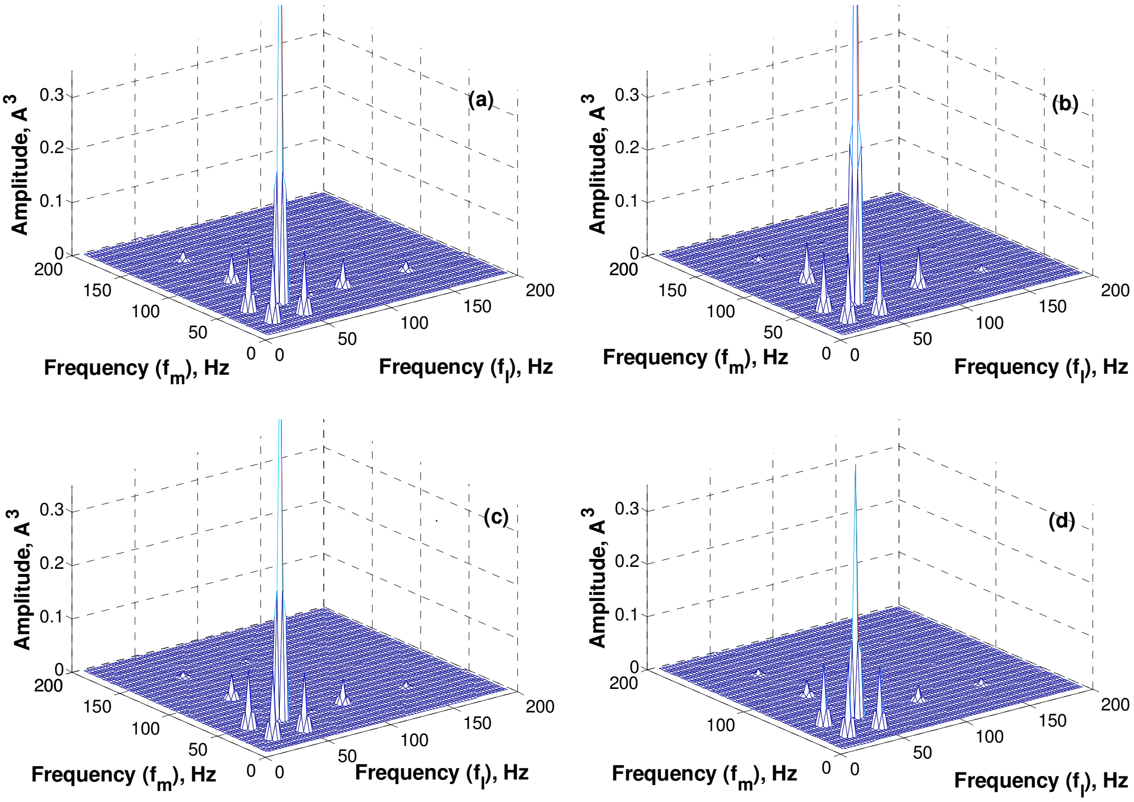

Figure 10 The bispectra of the stator phase current for the broken rotor bars motor, (a) No Load, (b) 25% Load, (c) 50% Load, (d) 75% Load

5.0. Conclusions

A method that can identify the fault in the motor at early stage and also capable to distinguish the rotor fault and the stator fault is always important so that the remedial action can be carried out quickly. Hence the use of the higher order spectra (HOS), namely the bispectrum has been tested and applied to the phase current signal of the motor for this purpose. The bispectrum is the tool which relates both amplitude and phase of number of harmonics in a signal. The motor phase current signal in case of any fault expected to contain number of harmonics components related to the motor RPM and the mains frequency. It is because any fault (either in the stator or the rotor) may distort the sinusoidal response of the motor phase current signal which results in number of harmonics of the motor RPM and the mains frequency. This has already been observed in the motor phase current spectra. But the amplitude spectra could not able to detect the rotor and the stator faults for the induction motor used in the experiments, however the bispectrum of the motor phase current successfully able to detect the stator and the rotor fault and also able distinguish the stator and the rotor fault which is considered to be useful information for fixing the problem quickly. Moreover, it has also been plan to test the trispectrum, other kind of the HOS, to observe possibility of the further improvement in the motor fault diagnosis.

Table 2 Comparison of the bispectrum components amplitude for different fault conditions for the motor when operating at 100% load

	Amplitude (Cubic Ampere, A^3) of Bispectrum Components				
	B_{11}	B_{22}	$B_{12} = B_{21}$	$B_{24} = B_{42}$	$B_{26} = B_{62}$
Healthy	0.025	2.70	0.020	0.080	0.018
Faulty Rotor	0.220	0.28	0.190	0.018	0.023
Faulty Stator (5 turn)	0.024	2.60	0.018	0.22	0.015
Faulty Stator (10 turn)	0.050	2.30	0.039	0.19	0.042
Faulty Stator (15 turn)	0.030	2.00	0.023	0.17	0.022

6.0. References

[1] Nandi, S., Toliyat, H.A., Li, X., Condition Monitoring and Fault Diagnosis of Electrical Motors—A Review, *Energy Conversion, IEEE Transactions* 20(4)(2005) 719 – 729.

[2] Schoen, R.R., Habetler, T.G., Effects of time-varying loads on rotor fault detection in induction machines, *Industry Applications, IEEE Transactions* 31(4)(1995) 900 – 906.

[3] Bellini, A., Filippetti, F., Franceschini, G., Tassoni, C., Kliman, G.B., Quantitative evaluation of induction motor broken bars by means of electrical signature analysis, *Industry Applications, IEEE Transactions* 37(5) (2001) 1248 – 1255.

[4] Ayhan, B., Chow, M.Y., Song, M.H., Multiple Signature Processing-Based Fault Detection Schemes for Broken Rotor Bar in Induction Motors, *Energy Conversion, IEEE Transactions* 20(2)(2005) 336-343.

[5] Henao, H., Razik, H., Capolino, G.-A., Analytical approach of the stator current frequency harmonics computation for detection of induction machine rotor faults, *Industry Applications, IEEE Transactions* 41(3)(2005) 801 – 807.

[6] G. Didier, E. Ternisien, O. Caspary, H. Razik, A new approach to detect broken rotor bars in induction machines by current spectrum analysis, *Mechanical Systems and Signal Processing* 21 (2007) 1127–1142.

[7] Kia, S.H., Henao, H., Capolino, G.-A., A High-Resolution Frequency Estimation Method for Three-Phase Induction Machine Fault Detection, *Industrial Electronics, IEEE Transactions* 54(4)(2007) 2305 – 2314.

[8] Marques Cardoso, A.J., Cruz, S.M.A., Fonseca, D.S.B., Inter-turn stator winding fault diagnosis in three-phase induction motors' by Park's vector approach, *Energy Conversion, IEEE Transaction* 14(3)(1999) 595 – 598.

[9] Bellini, A., Filippetti, F., Franceschini, G., Tassoni, C., Closed-loop control impact on the diagnosis of induction motors faults, *Industry Applications, IEEE Transactions* 36(5)(2000) 1318 – 1329.

[10] Tallam, R.M., Habetler, T.G., Harley, R.G., Stator winding turn-fault detection for closed-loop induction motor drives, *Industry Applications, IEEE Transactions* 39(3)(2003) 720 – 724.

[11] Henao, H., Martis, C., Capolino, G.-A., An equivalent internal circuit of the induction machine for advanced spectral analysis, *Industry Applications, IEEE Transactions* 40(3)(2004) 726 – 734.

[12] Aroquiadassou, G., Henao, H., Capolino, G.-A., Experimental Analysis of the dq0 Stator Current Component Spectra of a 42V Fault-Tolerant Six-Phase Induction Machine Drive with Opened Stator Phases, *IEEE International Symposium on Diagnostics for Electric Machines, Power Electronics and Drives (SDEMPED 2007)*, 6-8 Sept. 2007, pp 52 – 57.

[13] Nangsue, P., Pillay, P., Conry, S.E., Evolutionary Algorithm for Industrial Motor Parameter Determination, *Energy Conversion, IEEE Transaction* 14(3)(1999) 447-453.

[14] Huang, K.S., Kent W., Wu, Q. H., Turner, D.R., Parameter Identification of an induction Machine Using Genetic Algorithms, *Proceeding of the IEEE*

International Symposium on Computer Aid Control System Design, Hawai,1999, USA.

[15] Huang, K.S., Kent, W., Wu, Q.H., Turner, D.R., Effective Identification of Induction Motor Parameters Based on Fewer Measurements, *Energy Conversion, IEEE Transaction* 17(1)(2002) 55-60.

[16] Barut, M., Bogosyan, S., Gokasan, M., Speed-Sensorless Estimation for Induction Motors Using Extended Kalman Filters, *Industrial Electronics, IEEE Transaction*s 54(1)(2007) 272-280.

[17] Bachir, S., Tnani, S., Trigeassou, J-C., Champenois, G., Diagnosis by parameter estimation of stator and rotor faults occurring in induction machines, *Industrial Electronics, IEEE Transactions* 53(3)(2006) 963-973.

[18] Treetrong., J., Sinha, J.K, Gu, F., Ball, A.D., A Novel Model Parameter Estimation of an Induction Motor using Genetic Algorithm, *Proceeding of Signal and Image Processing ~SIP 2008~*. pp 623-015, 18-20 August 2008.

[19] Fackrel, J.W.A., White P.R., Hammond J.K., Pinnington R.J., Parsons T.A., The interpretation of the bispectra of vibration signals – I. Theory, *Mechanical Systems and Signal Processing* 9(3)(1995) 257-266.

[20] Collis, W.B., White, P.R., Hammond, J.K., Higher Order Spectra: the bispectrum and trispectrum, *Mechanical Systems and Signal Processing* 1998, 12(3)(1995) 375-395.